Revealing the Nature and Number of Active Centers on Metal Surfaces with Electrochemical Scanning Tunnel Microscope[1]

E. V. Kasatkin

State Scientific Center of the Russian Federation "Karpov Institute of Physical Chemistry,"
ul. Vorontsovo Pole 10, Moscow, 103064 Russia
e-mail: elchem@cc.nifhi.ac.ru.
Received February 9, 2004

Abstract—Measurements with scanning tunnel microscope are analyzed, as regards the relative number and properties of tunnel-active centers at metal surfaces (Pt single crystals, polycrystalline Rh, Pd, and Cu, highly oriented pyrolytic graphite, etc.), in particular, at controlled potential. The relative number and local properties of the tunnel-active sites, their tunnel conductance, and donor–acceptor properties are calculated. A tunnel exchange current observed, similar to the exchange current of electrochemical reactions, reflects reversible charge transfer across the interface showing equal rates of the forward and backward processes. A possible correlation between the tunnel and electrochemical stages of the charge transfer is discussed.

INTRODUCTION

Yakov Mikhailovich Kolotyrkin paid much attention to the development and application, in the Karpov Institute of Physical Chemistry, of novel, informative methods of studying corrosion-electrochemical systems and processes, in particular, the state of electrode surface. By means of electrochemical scanning tunnel microscopy (**ESTM**), we studied at a nanometer-scale level the nature and properties of surfaces of Pt(111), Pt(110), and Pt(311) single-crystal faces [1], as well as platinum–titanium (**PTTEs**) and iridium–titanium (**ITTEs**) textured electrodes. (The last two of them are industrial analogs of (111)-edged single crystals [2, 3].) Polycrystalline metals (Pd, Rh, Au, Cu) and some more complicated objects were also investigated [4–7]. Juvenile surface of highly oriented pyrolytic graphite (**HOPG**) served as reference (below we refer to the HOPG as graphite).

Undoubtedly, an advantage of the scanning tunnel microscope (**STM**) is its suitability for *in situ* studies of nanorelief (down to the atomic-size resolution) of conducting surfaces, in particular, at controlled potential. Additionally, local information concerning energy characteristics of the scanned areas can be obtained.

We should bear in mind that relief found by STM is not identical to that found by atomic-force microscope (**AFM**), because the former gives *electronic*, rather than geometrical (van der Waals) surface profile. STM measurements can be performed in either of two modes: with a stabilized (controlled) *preset tunnel current* I_{tc} (an I_t = const mode) or with stabilized *tunneling gap h* (a z = const mode).

In the first case (I_t = const), the STM electronic system, with preset and controlled *tunnel voltage* U_{tc}, continuously traces the tunnel conductance $G_{tc} = I_{tc}/U_{tc}$ and keeps I constant (equal to the preset value). For this purpose, the STM scanner continuously controls the tunneling gap h (corresponding to the current I_{tc}) between the STM tip and a site at the surface, above which the tip is arranged.[2] In this mode, the system continuously provides information on the relative position of the site over the conventional zero $Z = f(G_t, X, Y, \tau)$, where τ is the time and G_t is the local tunnel conductance.

In the second mode (z = const), the electronic system of STM keeps in memory the tip position in height in the initial moment of scanning, that is, the tunneling gap h corresponding to the preset current I_{tc} and voltage U_{tc}; it traces the further changes of the tunnel current I_t flowing through the tip, caused by changes in h over sites with different height Z, and provides the information $I_t = f(h, U_{tc}, X, Y, \tau)$.

At sites with abruptly raised or lowered G_t values, the value of I_t at the STM tip strongly declines from I_{tc}. The electronic system of STM, working in the mode I_t = const, generates a signal that immediately directs the tip up or down in order to restore the preset and controlled conductance G_{tc}. In the STM-image, a positive or negative overshooting can occur.[3] These overshoot-

---

[1] Presented at the 4th Session of All-Russian Conference on Corrosion and Electrochemistry (Ya.M. Kolotyrkin memorial), November 2003.

[2] In what follows, "site" means the point of the tunneling at atomic-size scale, down to tenths of angström, according to the STM resolving power with respect to the coordinates X and Y.

[3] The term "overshooting" means a single raise in h (the z-coordinate) in the STM-image over neighboring sites, which exceeds by a factor of 3 to 4 the atomic diameter for the studied material.

ings, when sharp and large, make the STM-image "less smooth." Therefore, most of experimenters use an automatic interference filtering mode in the STM software, thus loosing the objective information.

Our studies showed that the electronic nanorelief recorded by STM gives information on the sites with significantly raised tunnel conductance, indeed; these sites may correspond to active centers.

Identifying electrochemical active centers at the atomic-size scale with an STM is reasonable. The charge transfer rate is determined by height and width of energy barrier. Hence, both the electrochemical and tunnel currents must increase with lowering and narrowing the barrier. The term "active centers" that was introduced by A.A. Balandin [8] is now rarely used because some change in its initial meaning made it ambiguous [9]. In what follows, we discuss heterogeneous electrocatalytical processes, and the term "active center" implies the site at the surface, whose interaction with a reactant is significantly accelerated; however, a defect or adsorbed mediator species may not occur there. Numerous studies showed that the overall rate of electrochemical and corrosion processes is determined by elementary acts of the reaction occurring in a few active sites on the surface.

EXPERIMENTAL RESULTS

During 1995 to 2003, we performed complex STM- and scanning tunnel-spectroscopy (STS) studies of surface properties of variety of conducting materials, mostly of electrocatalytic nature [1–4]. Unfiltered STM-images of all these surfaces often have the overshootings, even if a few, marking significantly increased tunnel conductance. Therefore, we improved the procedure of PC-processing the STM data and the results of local nanocurrent–voltage measurements, to reveal quantitative characteristics of the studied surfaces. The percentage of the overshootings can be easily calculated, since we know the full number of discrete dots in the STM-image of a scanned area on the surface (mostly 2×10^4) and the number of the overshootings whose height, compared to neighboring area, exceeds 1 to 2 nm (often, even tens of nanometers). Other researchers also observed the overshootings (e.g., [10]), but have not analyzed and evaluated their nature.

To our view, the surface relief registered by STM reflects both the spatial structure of the surface and some features of its tunnel-electron activity, in particular, the centers of different activity and passivity, their distribution, and relative number. This number depends on the nature of material, axial orientation of the analyzed area, and adsorbed species, and, hence, the potential.

The overshootings may not be reliably observed within a small area (a few tens of square nanometers) constituted by less than one thousand atoms. However,

their observance appears more probable for larger areas (hundredths of square micrometer) with larger number of scanned atoms, when the surface scan step exceeds the atomic diameter (0.25 to 0.30 nm). Their number depends on the sample nature and potential, as well as electrochemical pretreatment, and other factors. At a repeated scanning, the overshootings have practically the same concentration but as a rule are registered at different sites. This evidences their energetic, rather than morphological, nature.

Probably, they reflect changes in the local electron concentration at some points of scanned surfaces, caused by fluctuations. Extremely defective spots show numerous overshootings. A preliminary analysis of the active sites was done in [1].

These overshootings are exemplified in Fig. 1 by STM-images of a PTTE[4] in 0.02 N H_2SO_4 at potentials from 0.40 to 1.12 V (vs. Ag,AgCl electrode). Figures 1b and 1c show difference between the surface images taken with and without the input-signal filtering at the same potential (0.8 V). The overshootings at the tunnel-active sites are darkened. Insert (Fig. 1f) shows a typical potential dependence of the active sites percentage found in this experiment with a platinum–titanium grain-oriented electrode.

In Fig. 2 we show STM-images of a single-crystal Pt(111) face, taken at a highest resolution. We see that a change in the sample potential from 1.31 V (2.50% of active sites, that is, practically the same concentration as at PTTE) to 0.30 V activated the surface drastically: 9.42% of active sites.

Our similar measurements performed with different electrode materials showed that the measured tunnel activity of the surface depends both on the potential and the electrode prehistory; it can vary from thousandths of percent to 10%. Figure 3 demonstrates the potential effect on the percentage of the tunnel-active sites for some electrode materials studied; the difference in their tunnel activity is clearly seen.

Unlike AFM, STM, and ESTM (electrochemical STM) methods allow performing local spectral measurements. An example of such measurements is the STS "in the voltage mode," namely, fixing tip over a preset site, switching to the "$z = const$" regime, sweeping the tunnel voltage bias U_t, at a scan rate v, from its initial value U_{tb} to the final value U_{te}, and recording the local current–voltage dependence $I_t(U_t)$.

The principles of quantum-mechanical nature of tunnel current are well substantiated. In numerous original papers, formulas are derived, which relate the tunnel current to the tunnel voltage. As an example, we

---

[4] The highly grain-oriented Pt-coating on Ti-substrate has axial 95%-(111)-texture; this is an industrial analog of the Pt(111)-face.
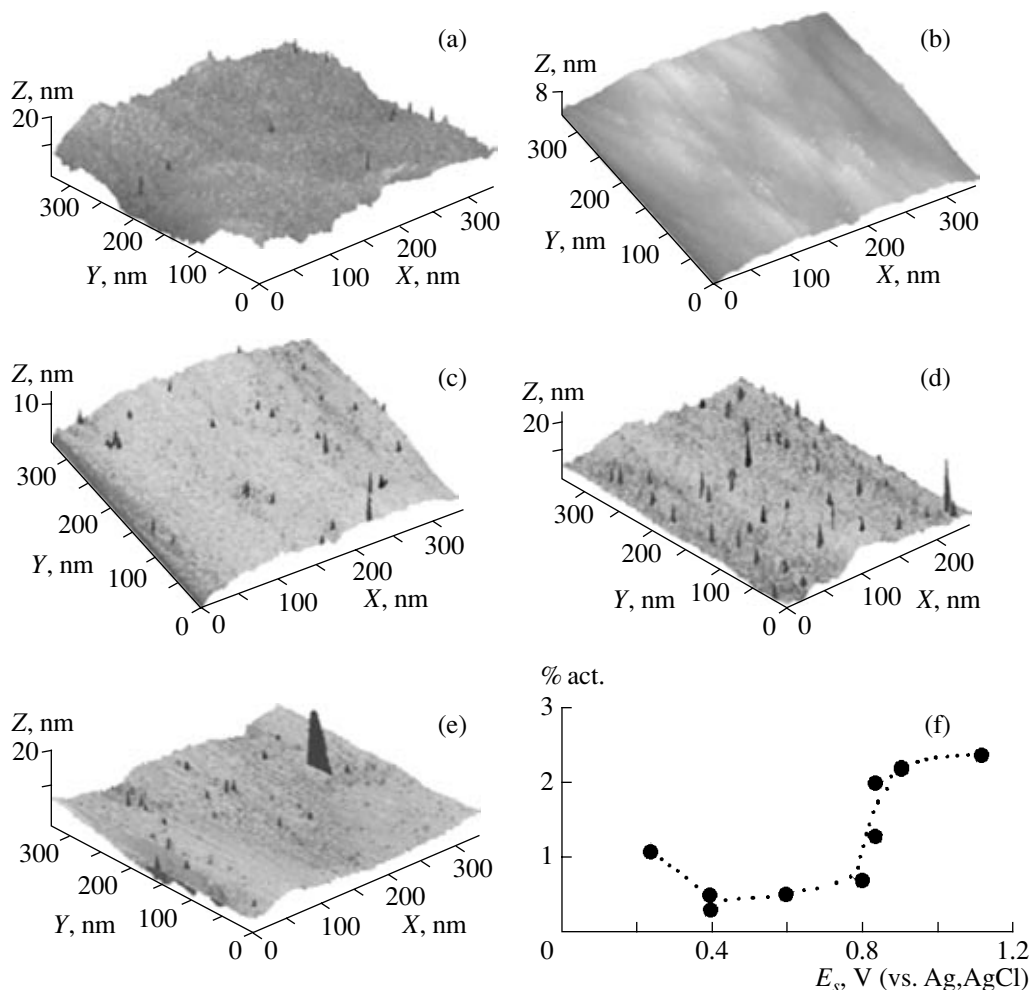
Fig. 1. Effect of potential and filtering on an STM-image of platinum–titanium grain-oriented electrode, an industrial analog of Pt(111)-edged single crystal, in 0.02 N H_2SO_4. The conditions of obtaining the STM-image: $I_{tc} = 0.840$ nA, $U_{tc} = 0.560$ V, scan rate 8.3 μm/s, scan step 2.61 nm, image field 341.74×336.50 nm; (b) with filtering, potential 0.8 V, no active site observed, height 8.0 nm; (a), (c), (d), and (e) without filtering: (a) potential 0.4 V, overshootings with height >2.6 to 13.09 nm—0.51%, height 18.243 nm; (c) potential 0.8 V, overshootings with height >2.4 to 11.1 nm—0.71%, height 13.416 nm; (d) potential 0.91 V, overshootings with height >1.2 to 12.8 nm—2.20%, height 10.14 nm; (e) potential 1.12 V, overshootings with height >2.7 to 12.1 nm—2.37%, height 9.14 nm; (f) the potential effect on the percentage of active sites in this experiment.

give the formula [11]:

$$i = \frac{2\pi e}{\hbar} \iint d^3 k_m d^3 k_t |H_{mt}(k_m k_t)|^2 \qquad (1)$$
$$\times [f(\varepsilon_t) - f(\varepsilon_m)] \delta(\varepsilon_t - \varepsilon_m - e\nu).$$

In this formula, index t is related to a tip; index m, to a substrate.[5] The last cofactor under the double integral (in the parentheses) points to the dependence of the tunnel current i on the tunnel voltage ν. The absolute value of i is also determined by the effect of Fermi levels ε and $f(\varepsilon_t)$ and $f(\varepsilon_m)$ on the Dirac distribution functions, as well as the effect of the matrix elements H_{mt} describing the interaction between the substrate and the tip orbit-

[5] We retained the notation of [11]; the symbols differ from those we used for the tunnel current (I_t), tunnel voltage (U_t), and tunneling distance (H).

als. The effect of the tunneling distance d is also significant. The above formula does not give explicitly the type of the $i(\nu)$ dependence [an equivalent of the $I_t(U_t)$ dependence]. Knowing all these parameters, one can calculate the tunnel current. However, we see that the above formula is too complicated to allow practically solving the reverse problem, that is, the calculation of these parameters by analyzing the experimental dependence $i(\nu) = I_t(U_t)$. In another form of the $I_t(U_t)$ dependence, suggested in [12], the tunnel voltage U_t appeared in the exponent in a power of 1/2. Evidently, the tunnel conductance G_t, which is a derivative dI_t/dU_t, should tend to infinity at $U_t = 0$, which is physically meaningless.

We found that the $I_t(U_t)$ spectra, like the Tafel curves in electrochemical and corrosion systems, become lin-
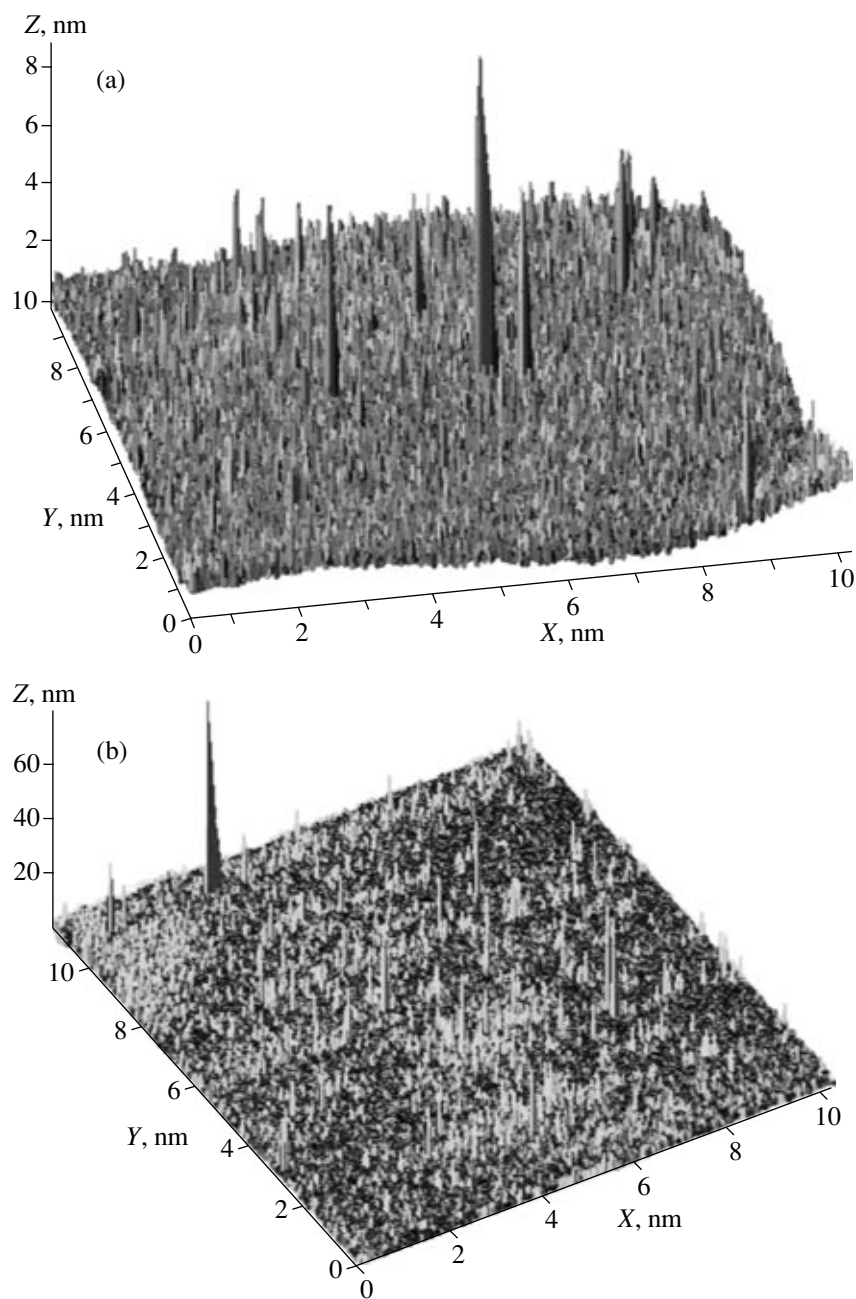
Fig. 2. STM-image of Pt(111) in 0.02 N H_2SO_4. The conditions of obtaining the STM-image: I_t = const = 0.940 nA, U_{tc} = 0.450 V, scan rate v = 3.0 μm/s, scan step 0.0365 nm; (a) potential 1.314 V, image field 10.3 × 10.91 nm, height 12.3 nm; (b) potential 0.315 V (after switching over from 1.314 V), image field 10.3 × 11.4 nm, height 79.6 nm.

ear when plotted in semilogarithmic coordinate system. This allows approaching the quantitative evaluation of the factors depending on the local tunnel activity of the sites. In this frame of axes, linear plots of the positive and negative branches of the tunnel current cross at U_t = 0, and the tunnel current in the crossing point is comparable with I_{tc}. This shows that the system is characterized by a *tunnel exchange current* I_{te}, which is proportional to the *minimal tunnel conductance* at U_t = 0 (G_0);

it depends both on the tunnel gap h and the site's local activity.

Based on the analysis of several thousands of $I_t(U_t)$-curves recorded on different materials, we concluded that the tunnel current can be well described by a simple empirical dependence:

$$I_t = I_{te}\{\exp(\alpha U_t G_0/I_{te}) - \exp[-(1-\alpha)U_t G_0/I_{te}]\}. (2)$$

where I_{te} is the tunnel exchange current, G_0 is the min-
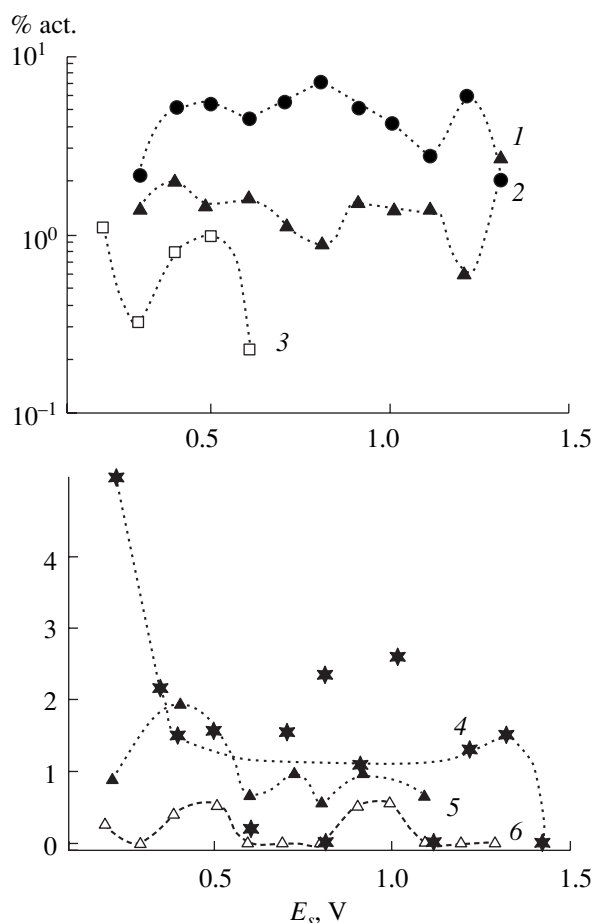
Fig. 3. Effect of potential on the relative number of tunnel-active centers at single-crystal Pt faces: (*1*) (311); (*2*) (111); (*3*) (110); (*4*) polycrystalline Rh; (*5*) platinum–titanium grain-oriented electrode; (*6*) platinum–iridium grain-oriented electrode.

imum tunnel conductance (both are defined at $U_t = 0$), and α is the transfer coefficient; these three quantities are physically obvious parameters. The dimensionless coefficient α characterizes the asymmetry of slopes of the positive branch dominated by the process of electron transfer to the tip and the negative branch of the $I_t(U_t)$ dependence dominated by the reverse process.

The common cofactor, the tunnel exchange current I_{te}, reflects the rate of reversible electron transfer in the tunnel contact in the absence of tunnel voltage, that is, the setting-in rate of an equilibrium not distorted by U_t. Noteworthy is that the possibility of occurrence of the tunnel exchange current is implicitly reflected in quantum-chemical formulas too. For example, we see from formula (1) that the tunnel current tends to zero when e_t equals $(e_m + e\nu)$, despite that its summands (depending on e_t and e_m) may not equal zero. These quantities constitute the tunnel exchange current; yet nobody has realized this before, to our knowledge. The ratio I_{te}/G_0 that appears in Eq. (2) and has dimension of voltage formally is similar to the coefficient RT/F appearing in the equations of electrochemical kinetics. The coefficient α quantitatively reflects the probability of electron transfer directed to the tip, which is determined by the donor–acceptor properties of the tip/sample couple.

It is obvious that the smaller the tunneling distance h (an analog of d in the notation adopted in [11]), the easier is the electron tunneling, and, hence, the higher the G_0 and I_{te} should be. We recall that the h value kept constant during scanning the surface in the STM mode (in the X axis direction with growing Y, or in the Y axis direction, with growing X), depends on the selected mode. When $I_t = const$, the h value is determined by the controlled tunnel conductance $G_{tc} = I_{tc}/U_{tc}$ (preset by experimenter). Here I_{tc} is the controlled tunnel current corresponding to the tunnel voltage U_{tc}. The distance h is continuously adjusted by the microscope feedback: the higher the G_{tc} the lower the h. When the local tunnel conductance G_t at a site lowers, the tip approaches the surface (thus decreasing h); when G_t grows, h increases. This is shown by STM as changing the height Z.

The difference between formulas (1) and (2) is that in (2), the parameters affecting the tunnel current are reduced to experimentally measurable coefficients (the tunnel conductance, the tunnel exchange current, and the coefficient characterizing the donor–acceptor properties of the tip and the sample). By processing experimental local spectra $I_t(U_t)$, all these parameters can be calculated [4].

It was shown that the independent quantitative information on the local tunnel conductance, in particularly at the atomic-size scale, can be obtained from measurements conducted in the STS mode; this cannot be done using other methods [1, 4, 13, 14]. Our calculations showed that when the tunnel gap is small enough (so that $G_{tc} > 1$ nS) the tunnel exchange current I_{te} appears comparable to I_{tc} and even several times larger. Therefore, the tunnel exchange current can significantly affect the positive and negative branches of the curves $I_t(U_t)$. We concluded that, like in electrochemical systems at a reversible potential, *at any U_t, a continuous charge transfer to and fro occurs between single atoms of the conducting surfaces that are in a tunnel contact*. In other words, a high-frequency electron exchange occurs. The exchange frequency of 10^{11} to 10^{13} Hz corresponds to typical I_{tc} values of 0.1–10 nA at $U_{tc} = \pm(0.1–1.0)$ V [4, 13, 14].

In active centers with elevated tunnel conductance G_0, the slope of the $I_t(U_t)$ curves abruptly increases at zero U_t; the tunnel transfer coefficient α often approaches unity, which corresponds to anomalous enhancement of the sample's donor properties at this site. Values of G_0, I_{te}, and G_0/G_{tc} also appear elevated. The opposite is true for passive sites: α approaches zero, and the G_0/G_{tc} value is very small. We see that the $I_t(U_t)$-spectra clearly reveal active and passive sites at the studied surfaces.
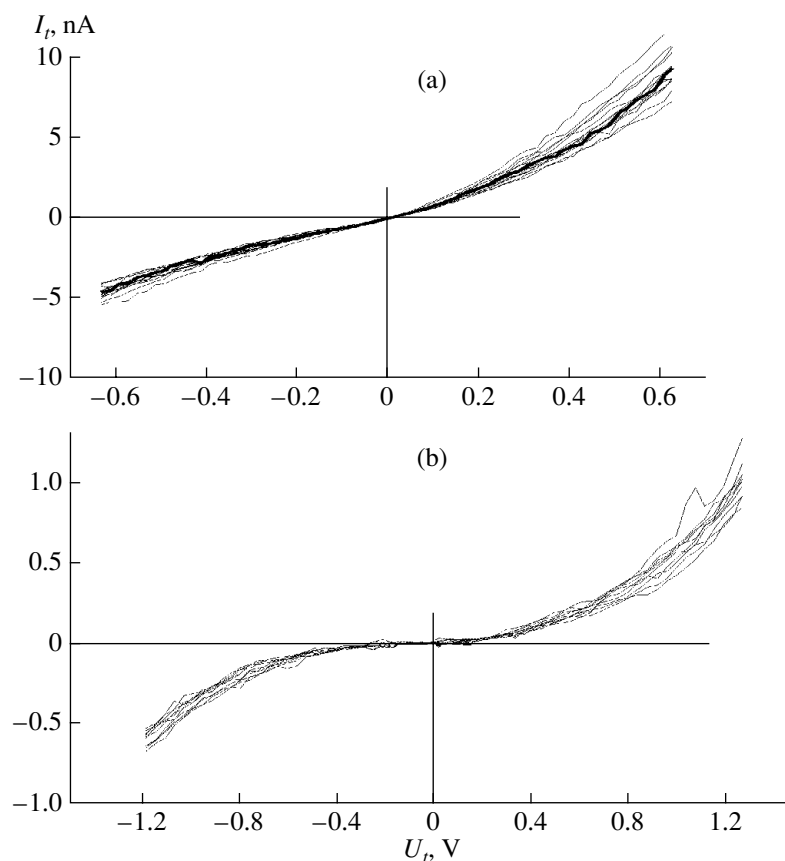
Fig. 4. Typical $I_t(U_t)$-spectra at HOPG (graphite) surfaces: (a) graphite/air. Experimental conditions: $I_{tc} = 0.50$ nA, $U_{tc} = 0.12$ V, $G_{tc} = 0.417$ nS. Scanning the spectrum along a line (38 sites) with a step of 0.037 nm, $v = +0.60$ V/s. The result of the experiment: $G_0 = 7.479 \pm 0.19$ nS, $I_{tc}/I_o = 288\%$, $I_{tc}/G_0 = 193 \pm 5$ mV, $\alpha = 0.629 \pm 0.005$; (b) graphite/vacuum. Experimental conditions: pressure 1.33×10^{-8} Pa, $I_{tc} = 2.3$ nA, $U_{tc} = 1.5$ V, $G_{tc} = 1.53$ nS, tungsten tip. Scanning of the spectrum (9 curves) in one point, $v = -31.6$ V/s. The result of the experiment: $G_0 = 0.156 \pm 0.16$ nS, $I_{tc}/I_o = 1.23\%$, $I_{tc}/G_0 = 181 \pm 18$ mV, $\alpha = 0.540 \pm 0.060$.

The number of such spectra recorded usually in a single experiment is incomparably smaller than the number of sites constituting an STM-image (hundreds of thousands). Hence, the percentage of active sites at the surface cannot be reliably calculated from the STS measurements "in the voltage mode." Moreover, experimenters often record the spectra at some specific areas in STM-images, rather than at occasional spots. This is one more reason for disagreement between the STM and STS measurements "in the voltage mode" when determining the percentage of active sites. Yet, usually surfaces with elevated (according to STM data) activity show increased number of "active" $I_t(U_t)$-curves.

An example of such $I_t(U_t)$-curves has been reported in [1] for single-crystal Pt-surfaces. Other examples given in Figs. 4 and 5 are rather typical curves for HOPG in air or in high vacuum and our data obtained with polycrystalline Rh-electrode in a 0.1 N H_2SO_4 at potential 0.5 V are shown.[6]

The curves in Fig. 4 are typical of "quiescent" graphite surfaces with practically no active centers. They are recorded by scanning with minimal step (several local curves within atomic dimensions) and reflect fluctuations of G_0 caused by the tip motion over different points in the electronic profile of an atom.

Figure 5 reveals the sites of higher tunnel activity in the spectrum. In Fig. 5a, a series of 24 $I_t(U_t)$-curves recorded in the middle of an STM-image at linear motion over the surface at a step of ~1.5 nm is shown. In this experiment, the STM-image contained 0.395% of active overshootings exceeding 17 nm and 2.73% of those exceeding 0.5 nm. The sites nos. 18 and 23 missed these "high overshootings."[7] The $I_t(U_t)$-curves mostly had a low slope, they practically merged up. Only two curves in this series (sites nos. 18 and 23) demonstrated a significantly elevated tunnel conduc-

---

[6] The experimental data for HOPG obtained with the use of a high-vacuum STM are courteously granted by M.V. Grishin (Semenov Institute of Chemical Physics, RAS) [14].

[7] When an $I_t(U_t)$-curve crosses such a "high overshooting" in the STM-image, it is so steep that the number of points in the vicinity of $U_t = 0$ appears insufficient to accurately calculate the parameters. Such curves were not processed by the adopted PC-program; the α values often exceeded 0.98 (see above).
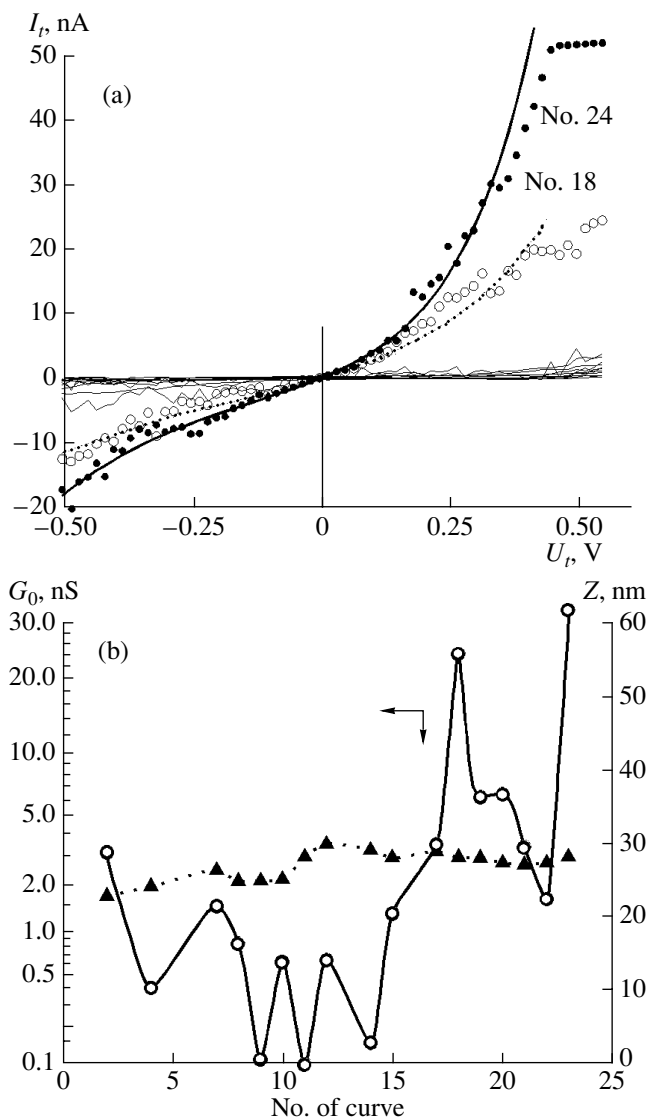
Fig. 5. The $I_t(U_t)$-spectra obtained at polycrystalline Rh electrode in 0.1 N H_2SO_4 at potential 0.5 V and the results of their processing: (a) a series of 24 $I_t(U_t)$-curves obtained by scanning STM-image along a line with the sites' coordinates $X = 50$ to 73, $Y = 73$ ($x = 75.776$ to 109.117 nm, $y = 114.466$ nm from the edge of the STM-image), step 1.516 nm, tip potential varied from 0.000 to 1.050 V (vs. Ag,AgCl) at a rate of $v = 0.66$ V/s; (b) ○ local tunnel conductance G_0 of the sites, ▲ their height Z (nm). The conditions of the STM measurements: $I_{tc} = 1.010$ nA, $E_{tc} = 0.445$ V, $E_s = 0.507$ V, $U_{tc} = -0.062$ V. Scan rate $v = 158.4$ nm/s in Y direction, negative drift –0.00299 nm/s during the period of 201.41 s, the field of STM-image 221.27 × 233.70 nm, the height drop 33.2610 nm, $N_x = 146$ sites, $N_y = 147$ sites.

tance. Figure 5b gives calculated G_0 values for different sites in this line in the STM-image. We see that these values are low for the majority of curves, even if varying from 0.1 to 2.4 nS. In Fig. 5a, we show curves calculated for the sites nos. 18 and 23 from the coefficients G_0, I_{te}, and α. When ignoring the curves nos. 18 and 23,

we obtained the following average values: $G_0 = 1.267$ nS, $I_{te} = 0.132$ nA, and α = 0.45. While for the active sites nos. 18 and 23, a 20 times higher value of $G_0 = 24$ nS is obtained; other parameters are: $I_{te} > 3.15$ nA, α > 0.65. A plot of the height profile Z for all points in this line of the STM-image is given in the same figure; we see no distinct effect of the surface profile on this drastic gain in activity.

The spectra shown in Figs. 4a and 5 were recorded during the STM measurements in air; those of Fig. 4b, in vacuum. Their form does not depend on the direction of potential scanning. Similar dependences obtained during STS measurements "in the voltage mode" in electrolyte solutions (in the potentiostatic mode) differ in that they reflect the effect of not only the tunnel voltage U_t and the sample potential E_s but also the direction of the tunnel scanning (because of changes in the STM-tip potential). Indeed, both E_s and the initial tip potential in the electrolyte E_{tc} affect the surface state and make marked changes in the adsorption layer. Such dependences exemplified by measurements with the iridium–titanium textured electrodes were discussed at length in [4].

In Fig. 6, we show histograms for the G_0/G_{tc}, α, and I_{te}/G_0 distributions. These parameters characterize the shape of the $I_t(U_t)$ spectra calculated by processing several series of data obtained with polycrystalline Cu, Pd, Rh, and graphite in air with the use of formula (2).

The polyextreme shape of distribution most strongly manifests itself for the parameter I_{te}/G_0. Most probably, it reflects the presence of surface states with different properties caused by adsorption of various oxygen-containing species, which can lower the effective tunneling barrier by several times [1, 11]. The mean values of α clearly differ for different materials. The nature of this effect is discussed in [4]. Rh exhibits most uniform α distribution. On the other materials, α distribution points to the presence of significant number of sites with lowered donor properties.

Because the G_{tc} values were different in different experiments, it is the G_0 to G_{tc} ratio that provides information necessary to evaluate the activity. Despite a significant scatter, on average, the values G_0/G_{tc}, tend to unity. In other words, the tunnel conductance on the surface at $U_t = 0$ and U_{tc} is on average the same. That is, *at a constant tunnel gap, the conductance insignificantly depends on the field applied and is determined by local surface properties*, which affect the scattering. When $G_0/G_{tc} > 2$, the curve is classified as *noticeably active*; when $G_0/G_{tc} > 10$, *very active*, that is, characteristic of anomalously elevated conductivity. When $G_0/G_{tc} < 0.7$, the site is classified as *passive*. Similarly, α > 0.85 and α < 0.15 were adopted as active and passive, respectively. These values, along with the data on the activity derived from the ratio G_0/G_{tc}, are summarized in table.
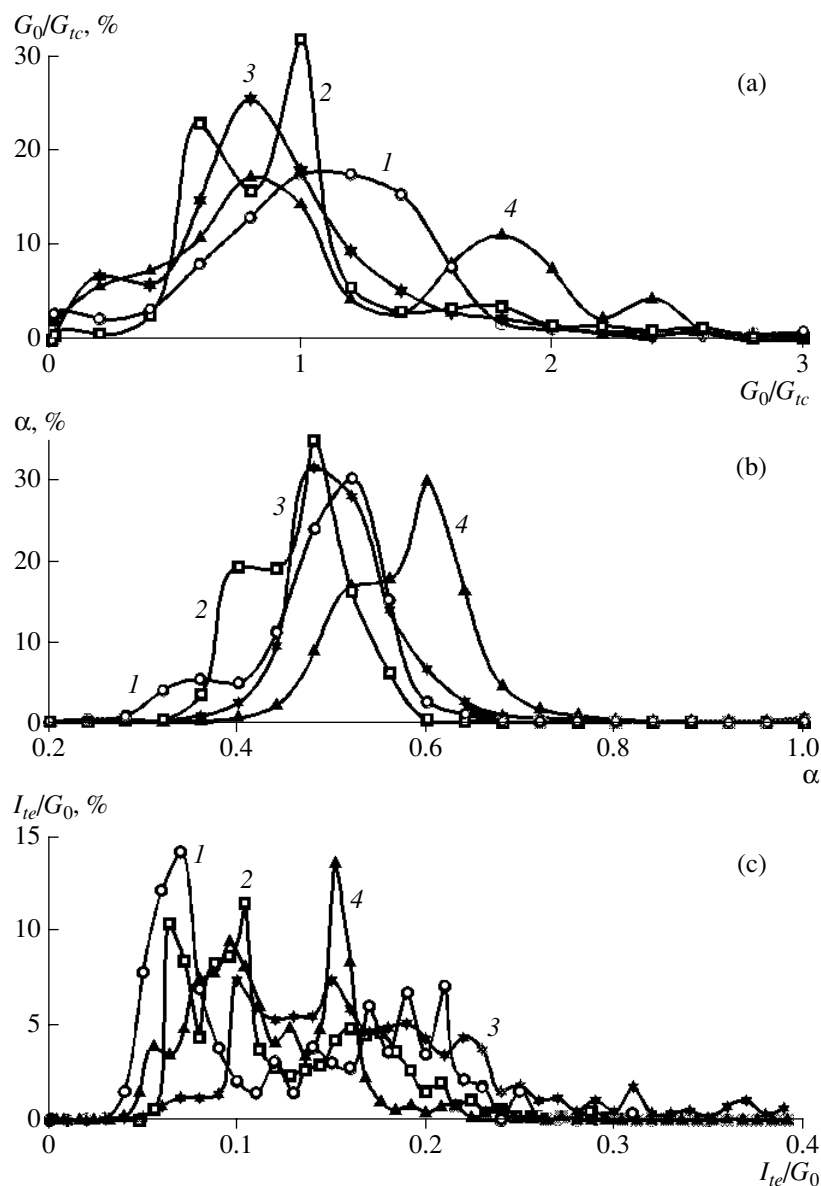
Fig. 6. Histograms of parameter distributions of Eq. (2) related to Cu, Pd, Rh, and graphite surfaces studied by STS "voltage mode": (a) relative tunnel conductance G_0/G_{tc}; (b) donor–acceptor activity coefficient α; (c) value of I_{te}/G_0, an analog of the Tafel coefficient b. Curves: (*1*) Cu, (*2*) Pd, (*3*) Rh, and (*4*) graphite.

As regards I_{te}/G_0, its average value (calculated, like the rest of the parameters, with weight factors) approaches 120 mV for graphite, Pd, and Cu, and is nearly twice as large for Rh. A maximum is observed at ~60 mV for copper and palladium. These values are close to typical slopes of Tafel current–voltage lines, and this suggests some ideas.

Effects of the sample material on the percentage of active and passive sites detected by processing $I_t(U_t)$-curves

Material	$G_0/G_1 \geq 10*$	$G_0/G_1 \geq 2**$	$G_0/G_1 < 0.7***$	α_{act}	α_{pass}	I_{te}/G_0, V
	%					
Graphite	0.814	16.35	25.83	0.7924	0.0010	0.1193
Rh	0.545	8.70	28.07	16.92	1.1260	0.1987
Pd	0.814	10.15	26.71	0.0000	0.0405	0.1241
Cu	1.541	10.72	16.41	0.3101	0.1919	0.1318

  * *Very active*, for which $G_0/G_{tc} > 10$.
 ** *Rather active*, for which $G_0/G_{tc} > 2$.
*** *Passive sites*, for which $G_0/G_{tc} < 0.7$.

CONCLUSIONS

Strongly correlated results of STM and STS measurements allow evaluating the number and properties of active centers at electrocatalysts' surfaces, namely, local (at the atomic-size scale) and averaged tunnel activity and its quantitative characteristics: the relative tunnel conductance G_0/G_{tc} and the coefficient α characterizing the local donor–acceptor properties of surfaces. STS "in voltage mode" appears to be the most effective method of determining the above parameters reflecting at atomic level the basic properties of conducting surfaces, whereas traditional STM-images (without prefiltering) may be used to easily and quantitatively evaluate the percentage of active centers.

On discussing the data that evidence the possibility of recording and quantitatively evaluating the centers with elevated tunnel activity at metal surfaces, we cannot ignore the question whether this information correlates with the data on the active centers in the electrochemical systems. The tunnel currents are negligibly small. In electrochemical reactions exchange currents are much higher, and charge transfer proceeds directly between the contacting atoms. The contribution from the negligibly small tunnel currents is seemingly insignificant, and studying the nanoampere-scaled tunnel processes may seem unreasonable.

To resolve the question, the corresponding current densities should be compared.

In electrochemical processes, current densities in a range from 10^{-8} to 10^2 A/cm^2 are dealt with; the exchange currents are of the same order [15]. In aforementioned results of STM measurements, the tunnel current I_t and the exchange current I_{te} are not reduced to unit surface; they correspond to recorded rate of a process between the tip and a single atom at the surface under study. To accurately compare the tunnel current with an electrochemical one, the range of recorded tunnel current densities should be estimated. For example, 1 cm^2 of flat polycrystalline platinum surface contains nearly 1.3×10^{15} atoms, Pt(111)-face, up to 1.49×10^{15} atoms. Multiplying correspondingly a tunnel current of 1 nA results in a current density of 0.77×10^6 or 0.67×10^6 A/cm^2, that is, four orders of magnitude higher than the maximum current density electrochemists deal with. Here is the problem.

Firstly, theoreticians involved in electrocrystallization took into account its crystallographic aspects as long ago as in 1930s (and Ya.M. Kolotyrkin, as regards corrosion, in 1960–1970s). They realized that at any moment the number of active surface sites (centers), where elementary act of dissolution of an atom is physically possible, is negligibly small compared with their total number. Secondly, an overbarrier charge transfer of reacting species in electrochemical reactions is still hypothetic, because it has not been proved for the elapsed 75 years. At the same time, nobody disproved of calculations based on the hypothesis of tunnel transfer. We classify our supposition as disputable (that is requiring further investigation). Such a discussion will help in answering the question: why the coefficients α and β in equations of the electrochemical kinetics remain virtually constant in a potential range up to several volts, despite the inevitable changes in the shape of the potential barrier. Evidently, when the potential energy curves are shifted to the positions corresponding to a barrierless or activationless process, the contribution from tunnel conductance must decrease sharply, which prevents the coefficients α and β from remaining constant; they must come to values of ~1 or ~0.

Why then the coefficient I_{te}/G_0 recorded in STS measurements (Fig. 5), and tantamount to the slope b, whose mean value approaches the Tafel slope, varies over wide range, unlike more stable slope b measured in electrochemistry? May be the coefficient I_{te}/G_0 reflects *the local properties* of the barrier overcame by a charge in each elementary act, whereas b is averaged over 10^{11} to 10^{15} atoms, so that all local differences appear absolutely imperceptible, even in measurements with microelectrodes. It is not improbable that subbarrier tunnel electron transfer may appear an important stage in the majority of electrochemical reactions.

I believe that these suggestions are worth noting, no matter how strange they are at first sight. The problem of studying the role of tunnel currents in electrochemical processes is ripe; and calls for involvement of both experimenters and theoreticians.

To conclude, I should remind that Yakov Mikhailovich Kolotyrkin always displayed great interest to any novel, insufficiently studied problem that calls for new understanding of the corrosion-electrochemical processes.

REFERENCES

1. Kasatkin, E.V. and Neburchilova, E.B., *Elektrokhimiya*, 1998, vol. 34, no. 10, p. 1154.

2. Kasatkin, E.V. and Neburchilova, E.B., *Elektrokhimiya*, 1996, vol. 32, no. 8, p. 917.

3. Neburchilova, E.B. and Kasatkin, E.V., *Elektrokhimiya*, 2000, vol. 36, no. 12, p. 1448.

4. Kasatkin, E.V., Reznik, M.F., and Neburchilova, E.B., *Elektrokhimiya*, 2003, vol. 39, no. 3, p. 265.

5. Abstracts of Papers, *Mezhdunarodnaya konferentsiya "Elektrokataliz v elektrokhimicheskoi energetike"* (International Conference "Electrocatalysis in Electrochemical Energetics"), Moscow: Russian Research Center Kurchatov Institute, 2003.

6. Bogdanovskaya, V.A., Tarasevich, M.R., Kuznetsova, N.N., *et al.*, *Biosensors Bioelectronics*, 2002, vol. 17, p. 945.

7. Kasatkin, E.V., Romashin, S.N., Sedov, A.V., and Kharlamov, V.F., Abstracts of Papers, *12 konferentsiya po radiatsionnoi fizike i khimii materialov* (12th Conference on Radiation Physics and Chemistry of Materials), Tomsk, 2003.

8. Balandin, A.A., *Mul'tipletnaya teoriya kataliza* (The Multiplet Theory of Catalysis), part 1, Moscow: Mosk. Gos. Univ., 1963.

9. Ashmore, P.G., *Catalysis and Inhibition of Chemical Reactions*, London: Butterworths, 1966.

10. Funtikov, A.M., Lunke, U., Stimming, U., and Vogel, R., *Surf. Sci. Lett.*, 1995, vol. 324, p. L343.

11. Claypool, C.L., Faglioni, F., Goddard, W.A., III, *et al.*, *J. Phys. Chem. B*, 1997, vol. 101, no. 31, p. 5978.

12. Halbritter, J., Repphun, G., Vinzelberg, S., *et al.*, *Electrochim. Acta*, 1995, vol. 40, p. 1385.

13. Kasatkin, E.V., Reznik, M.F., and Neburchilova, E.B., Abstracts of Papers, *13 Simpozium "Sovremennaya khimicheskaya fizika" (Tuapse, 2001)* (13th Symposium "Modern Chemical Physics"), Moscow: Mosk. Gos. Univ., 2001, p. 92.

14. Kasatkin, E.V., Reznik, M.F., Neburchilova, E.B., and Grishin, M.V., Abstracts of Papers, *14 Simpozium "Sovremennaya khimicheskaya fizika" (Tuapse, 2002)* (14th Symposium "Modern Chemical Physics"), Moscow: Mosk. Gos. Univ., 2002, p. 83.

15. *Spravochnik po elektrokhimii* (Reference Book on Electrochemistry), Sukhotin, A.M., Ed., Leningrad: Khimiya, 1981.